Fluorescence Enhancement from Individual Plasmonic Gap Resonances

Marcus Schmelzeisen, Yi Zhao, Markus Klapper, Klaus Müllen, and Maximilian Kreiter*

Max-Planck-Institute for Polymer Research, Ackermannweg 10-55128 Mainz, Germany

ARTICLE

ABSTRACT We studied the fluorescence enhancement of a dye-loaded polyphenylene dendrimer in a gap of 2—3 nm between a silver film and single silver particles with an average diameter of 80 nm. This sphere-on-plane geometry provides a controllable plasmonic resonator with a defined dye position. A strong fluorescence signal was seen from all particles, which was at least 1000 times stronger than the signal from the plane dye-coated metal surface. The fluorescence emission profile varied between the particles and showed light emission at higher energies than the free dye, which we assigned to hot luminescence. The maximum fluorescence emission peak shifted along with the scattering maximum of the plasmonic resonance. Two classes of scattering resonators could be distinguished. Up to a significant line-broadening, the response of the "sphere-on-plane"-like cases resembled the theoretical prediction for a perfect sphere-on-plane geometry. Resonators which deviate strongly from this ideal scenario were also found. Electron microscopy did not show significant differences between these two classes, suggesting that the variations in the optical response are due to nanoscale variations of shape and roughness in the gap region. The strong modifications of the dye emission spectrum suggested the presence of physical mechanisms at very small metal/dye separations, which are beyond a simple wavelength-dependent enhancement factor.

KEYWORDS: surface-enhanced fluorescence · sphere-on-plane · gap resonance · localized plasmon · perylene · dendrimer · strong coupling · single objects · nanoparticles

The excitation and emission rate of electronic transitions in organic dyes near nanoscopically structured metallic objects can be greatly enhanced compared to those in the dye alone. These enhancement effects are exploited in surface-enhanced Raman scattering (SERS).[1,2] They can be used in sensor applications,[3,4] to increase the electro-luminescence of light-emitting diodes,[5,6] or to promote the conversion of light to electric current in solar cells.[7]

Fluorescence enhancement was first observed for several dyes adsorbed directly onto silver-island films.[8,9] The maximum luminescence yield was obtained when the dye absorption maximum coincided with the particle plasmon resonance absorption maximum, which could be shifted by varying the island film average mass thickness. Wokaun[10] provided a comprehensive overview on early work in the field. Two physical processes are assumed to be involved. First, the excitation rate of the chromophore is determined by the electrical field at its position. This field can be greatly enhanced by metal particles compared to the incident field. Second, the emission rate of the dye is also influenced by the metal. This leads to further effects: new decay channels are generated, which may not lead to detectable photons but to energy dissipation in the metal. In addition, the rate of emitted photons can be greatly increased.[11] The latter effect is, by reciprocity, closely connected to the local field enhancement.[12] As long as the enhancement factor remains moderate, the intrinsic excitation and emission spectrum of the dye remains unchanged. The fluorescence of the coupled dye—metal system can then be modeled by taking into account the excitation field enhancement and by convoluting the emission spectrum of the free dye with the wavelength-dependent enhancement of the emission due to the metal. In spite of good understanding of the involved processes, even for this weak-coupling regime, only limited experimental progress was made for quite a time. The reason was that samples with controlled metal structures and dye positions have not been available. To date, quantitative experiments as reported for a single particle interacting with a single dye[13,14] remain the exception rather than the rule.

Nanometer-sized gaps provide very large electromagnetic field enhancements. Double spheres[15,16] and sphere-on-plane geometries[17−19] possess such gaps with dimensions down to the sub-nanometer level. At the same time, their resonance wavelength can be easily tuned, *e.g.*, by

*Address correspondence to Schmelz@mpip-mainz.mpg.de, Kreiter@mpip-mainz.mpg.de.

Received for review November 19, 2009 and accepted May 12, 2010.

Published online May 19, 2010. 10.1021/nn901655v

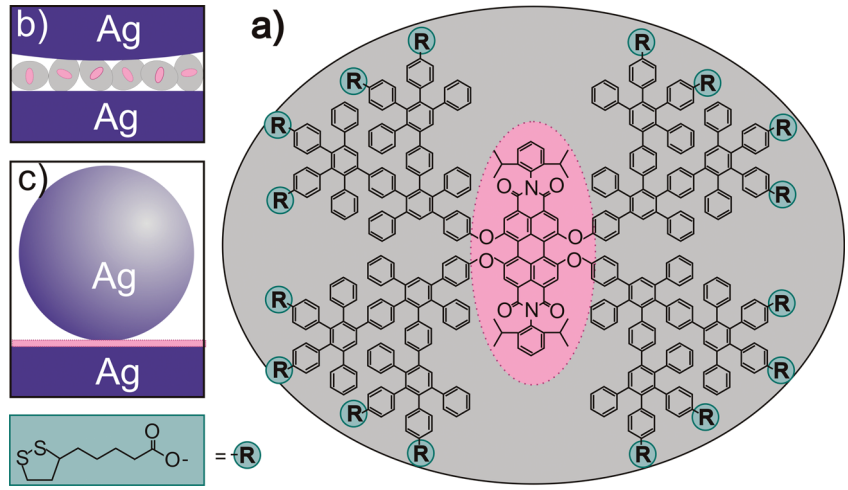

Figure 1. (a) Dendrimer PDI-G2, (b) sketch of the gap region, and (c) geometry of the sphere-on-plane system with a 3 nm spacer and 80 nm sphere (to scale).

changing the sphere diameter to match the molecules' excitation and emission wavelength. As a consequence, they are simple and highly efficient structures for fluorescence enhancement measurements. Quantitative experiments on these gap resonances are of great interest since they promise maximum enhancement factors. For small gaps of less than 3 nm, physical effects beyond the weak-coupling regime are expected, which represent the main motivation for the work presented here.

Already at moderate coupling the total decay rate of the excited electronic state can become comparable to the internal relaxation rate. The excited electrons in a vibrational level of the excited electronic state may then return to the ground state radiatively and not undergo thermal relaxation to a lower-energy vibrational level of the excited state from which they can make transitions to the ground state. This mechanism is called hot luminescence.[9] For very strong local field enhancements, which are possible for very small dye−metal separations, several additional physical effects should be taken into account. The local field effects may be strong enough to shift the transition frequency of the dye by a considerable amount.[12] Similarly, the dye may shift the plasmon resonance. The latter effect has been observed for dye ensembles on single plasmonic resonators.[20−22] Ultimately, coupling of single dyes to single plasmonic resonators may lead to a "strong coupling regime".[23] Here a quantum-electrodynamic description is required showing energy oscillations between the plasmon and the dye accompanied by a line splitting. On small length scales the description of the metal response as bulk dielectric breaks down. For subnanometer gaps between metal crystallites with a diameter of 2.5 nm, significant deviations from the calculation based on the bulk material response were shown.[24,25] Larger spheres with dielectric material in the gap are expected to show these deviations for gaps in the range of a few nanometers (Nordlander, personal communications). Instead of a full quantum treatment, corrections to the bulk metal response may be approximately described in the framework of a nonlocal (k-dependent) dielectric function, $\varepsilon(\omega,k)$.[26] In addition, surface states play a role.[27] Finally, at some stage the modeling of the chromophores as a point dipole must be replaced by a full quantum treatment for small dye−metal separations.[28] Truly quantitative experiments in these regimes require the defined placement of dyes relative to the enhancing metal structure.

In this article we introduce a silver "sphere-on-plane" (SOP) geometry which appears promising for this purpose. A perylene diimide-loaded polyphenylene dendrimer in generation 2 (PDI-G2) serves as both a spacer and a chromophore-bearing unit (Figure 1a). The dendrimer in the shell with only phenyl−phenyl linkages accounts for an outstanding rigidity and consequently exhibits shape persistency[29] while being optically inactive.[30] The 16 peripheral dithiolane rings establish the necessary affinity for binding to the silver substrate and the silver particles on top. The chromophore in the core can be accordingly placed with nanometer precision in the gap between the metallic structures. The selected perylene dye itself stands out in terms of photostability and fluorescence quantum yield.[31,32] On a single object basis we investigate the fluorescence from these structures and correlate this information with plasmonic resonances obtained by dark-field microscopy and the particle shape obtained by scanning electron microscopy. We find a reproducible enhancement as well as several spectral features which appear to be unique for the presented system. Although we cannot uniquely assign any of our observations to any described mechanism in the strong-coupling regime, the system shown provides several promising starting points for further experimental and theoretical investigation, and we regard this as an important step toward full quantitative experiments.

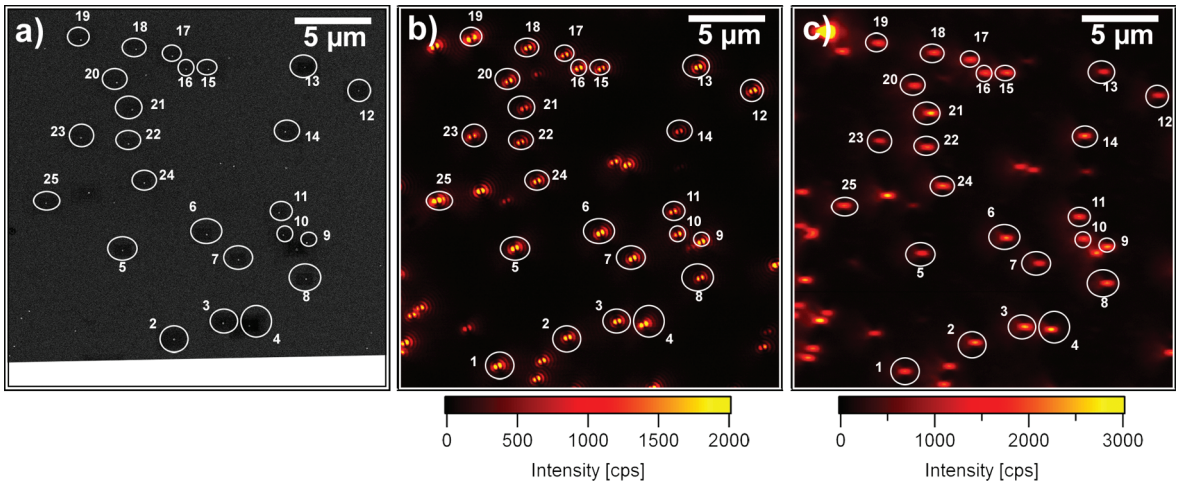

Figure 2. (a) Scanning electron micrographs of the area under investigation. (b,c) Corresponding fluorescence and scattering images.

RESULTS AND DISCUSSION

Figure 1 shows the SOP system with the perylene dye in the gap. A monolayer of the PDI-G2, as depicted in Figure 1a, covers the silver film and serves as a spacer for additional silver particles. Figure 1b illustrates the spacer region, with the dendrimers shown as elliptical particles. In Figure 1c, a to-scale sketch assuming a spacer layer of a thickness $d = 3$ nm and a silver sphere with a radius $r = 40$ nm is shown. Details on the preparation of silver SOP resonators, using the PDI-G2 as spacer layer, are given in the Experimental Section.

Figure 2a−c shows an area of 25 × 25 μm^2 seen by electron microscopy, scanning confocal fluorescence microscopy, and scanning dark-field microscopy. Note the excellent one-to-one correspondence between the white objects seen by electron microscopy (a) and the bright spots in fluorescence (b) and scattering mode (c) of the confocal microscope. These objects are identified as surface-bound silver particles by increasing the magnification in the electron microscope. Areas without particles show only very little fluorescence. This indicates that all dyes are very close to the surface since they are almost perfectly quenched if not decorated by a particle. A surface-bound silver particle on top leads to an effective "dequenching" of the dye, and visible radiation is emitted. All particles show a signal which verifies that dye molecules are located under each of them. In Figure 2c, the unusual bright spot in the top left, where there is no fluorescence in Figure 2b, is a depression in the silver film. A magnified image is available in the Supporting Information, Figure S3.

The particles in the fluorescence image show the typical patterns for dipoles excited normal (*z*-axis) to a metallic surface.[33] This response is expected for the vertical resonance of the SOP system, which is accompanied by a large field enhancement in the gap.[17−19] The scattering in Figure 2c can be assigned to *z*-dipoles as well.[34] They appear as individual dots in the particular imaging mode used here but can be uniquely identified as vertical dipoles since, upon illumination with the appropriate polarization, they display similar double-lobe patterns as in Figure 2b (see Supporting Information, Figure S6).

In order to quantify the optical response of these resonators, fluorescence and scattering spectra for 36 objects were recorded. A representative selection of fluorescence (red) and scattering spectra (black) is shown in Figure 3, together with the emission spectrum of the dye in solution for comparison (gray) and a magnified electron micrograph. All individual spectra are presented in the Supporting Information, Figures S7 and S8. The fluorescence signal of an uncovered position in the neighborhood is displayed as a reference (blue). It shows a sharp maximum originating from the illumination light. Scattering intensities are all scaled to the same value, while the fluorescence intensities are scaled for optimum visibility.

We distinguished two classes of resonators by visual inspection of the scattering spectrum. First are those showing two pronounced resonances around 450 and 600 nm, respectively, separated by a clear minimum. Around 50% of all particles (17 of 36) exhibit this behavior, which would be expected for spher-on-plane or at least SPO resonances. We group them into the category "SOP-like resonators". They are represented in Figure 3a−c. In Figure 3 d we illustrate a case which is ambiguous. It shows two clear peaks, but the long-wavelength peak at 530 nm is far blue-shifted relative to all SOP-like resonators. We decided not to assign it to this group.

A calculation for a silver SOP system with a homogeneous dielectric environment using the quasistatic model from Wind *et al.*[35] is displayed in Figure 4. The imaginary part of the polarizability displays a peak at 580 nm and some additional peaks at wavelengths shorter than 450 nm. They may be attributed to fundamental (longer wavelength) and higher order resonances.

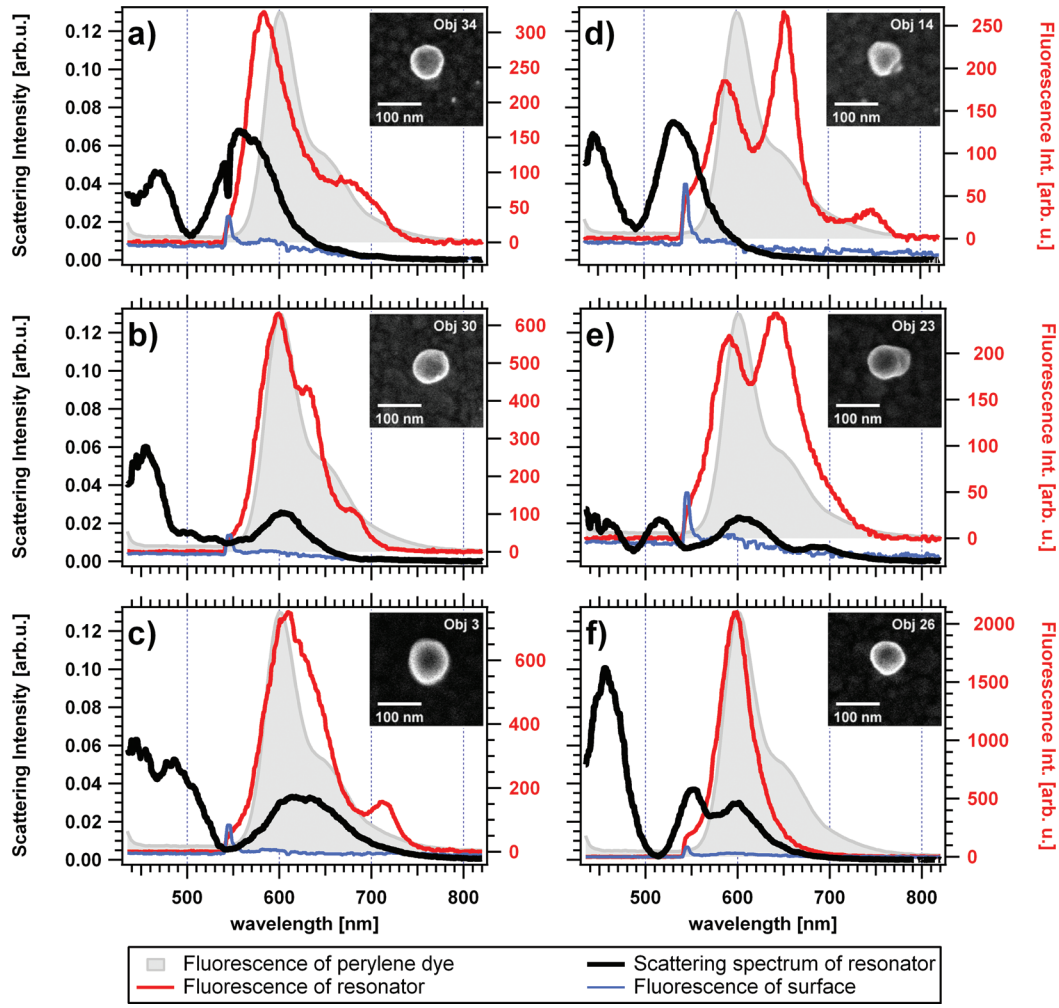

Figure 3. Fluorescence spectra from particle positions, compared to the background fluorescence signal. The emission spectrum from the dye in solution at an excitation wavelength of 405 nm is shown in gray. The black curves are all scaled to the same maximum value and show the scattering signal of the particles, which are presented at the top right.

Experimentally, the fundamental resonance is clearly seen in Figure 3a−c. The variations in peak wavelength from 560 to 640 nm are representative for all investigated particles. The different proportions of the fundamental and higher order peaks in theory and experiment are related to the wavelength-dependent response in plasmon-mediated dark-field microscopy, which decreases its efficiency with increasing wavelength. The full width at half-maximum (FWHM) for the fundamental resonance ranges from 57 to 98 nm in our experiments and is significantly more than theoretically predicted (15 nm). Since inhomogeneous broadening can be excluded for the single-particle experiments shown here, we observe a significant deviation of our system from the response expected for a perfect SOP system. While we can only speculate about the physical mechanisms, we note that this increased resonance width points to a lower quality factor of the resonance and therefore may result in much lower local field enhancements than suggested by calculations. We note that different values for the dielectric function of silver can be found in the literature. For example, in the book of Palik[37] significantly higher damping factors are quoted, leading to a calculated resonance width of 35 nm, more than double that found for the dielectric function stated by Johnson and Christy but still below our experimental values (see Supporting Information, Figure S9). Measurements of the dielectric function are necessarily performed on nonperfect samples

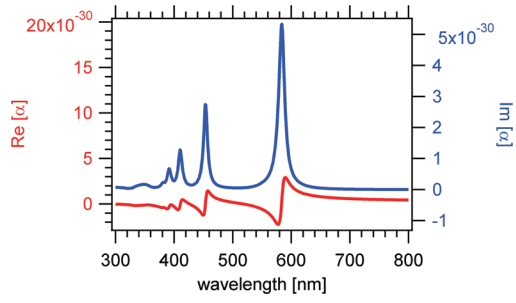

Figure 4. Calculation with Wind's equation[35] for a sphere with $r = 40$ nm and a homogeneous environment with $\varepsilon = 2.25$. The ε values for silver are from Johnson and Christy.[36]

and therefore can be regarded as an upper limit for damping.[38] Therefore, we consider the Johnson and Christy data to be the better choice.

The features seen experimentally below 500 nm are tentatively assigned to the higher-order peaks predicted by theory. Their positions show strong variations, but again they are much broader than predicted, with the same consequences as for the fundamental. We note that they do not contribute to the fluorescence enhancement, since they occur at a wavelength far away from the emission of the particular dye studied here.

Individuals with a scattering response which clearly differs from an ideal SOP resonance are shown in Figure 3e,f. In total, such a non-SOP-like response is found in 19 cases. More resonances at different wavelength positions are visible with no apparent correlation to the shape of the particles. These variations may originate from different shapes of the gap between the metallic structures, which is not accessible by our methods, and show, together with the large variation in peak wavelength for the "SOP-like" scatterers, the importance of a single object analysis.

The fluorescence spectra differ from the emission spectrum of the chromophore in solution. Of particular interest is the appearance of photons at wavelengths below 560 nm, where the free chromophore does not emit at all. This emission is reproducible not only for different individuals but also for different excitation wavelengths and different samples (see Supporting Information, Figure S10). This modification of the fluorescence emission spectra by coupling to plasmonic resonances is assigned to hot luminescence from higher vibrational levels of the electronic excited state.[9] It suggests that the PDI-G2 emission is enhanced to an extent that the electromagnetic decay rate is at least of the same order as the vibronic relaxation, which occurs on the picosecond time scale.

On the red side, above 700 nm, the emission spectra show in most cases less fluorescence than the free dye. This is true for 26 of 36 particles shown in the Supporting Information, Figure S7, most probably due to the absence of a plasmonic resonance at this wavelength region. In some cases additional fluorescence peaks appear on the red side of the spectrum. This observation cannot be explained in terms of hot fluorescence, which manifests itself in blue-shifted emission. This is a first hint for additional effects which have to be taken into account. For the SOP-like samples in Figure 3a−c, the fluorescence emission peak maximum shifts along with the scattering resonance from 593 to 609 nm. This can be experimentally understood in terms of a wavelength-dependent enhancement of the dye fluorescence by the plasmonic resonance, assuming that the scattering spectrum roughly represents the wavelength-dependent enhancement factor.[39,40] By taking into account the fluorescence originating from a dye-covered surface with and without particle and considering the focal and particle area, an average enhancement factor of around 1100 for the particle-covered dye in comparison to the strongly quenched dye on the silver surface is estimated. This very conservative estimate is explained in detail in the Supporting Information, section A11. Another important reference is the brightness of the unquenched chromophore. By comparison with single-molecule fluorescence data, we arrive at a brightness of the dequenched dye which is as high as that of a free dye far away from any metal, despite a nanometer scale proximity to silver (see Supporting Information, Figure S14, for details). For the non-SOP-like resonators the fluorescence signals show strong spectral variations. Both the strongest and the weakest fluorescing individuals are found in this class of resonators. The wavelength positions at maximum fluorescence vary from 588 to 650 nm. In particular we find clear emission lines at wavelengths which differ from resonator to resonator (see Supporting Information, Figure S11), where all emission spectra are compared. This behavior differs from the enhancement of individual transitions at a few well-defined wavelengths, as observed by Ringler *et al.*[40] There, the enhancement could be described in terms of a constant emission spectrum of the dye and a resonator-specific enhancement. Here, we see exclusively emission from the gap, where the perturbation of the dye by the nearby silver is so strong that the lines we see occur at wavelengths which are different from resonator to resonator. We cannot uniquely assign this remarkable feature to a specific physical effect. Strong coupling as discussed in the context of SERS[21,22] as well as strong spectral shifts due to a high local density of states (LDOS)[12] may play a role here. For these non-SOP-like resonators, an average enhancement factor around 1000 is calculated, taking the quenched dye as the reference. We note that light-induced fragmentation of the chromophores in the gap cannot be excluded at these high field enhancements, though the accelerated emission is known to balance this effect and lead to an enhanced stability. Finally, one has to rely on experimental evidence that the system is stable and that the spectral variations are not due to photoproducts. We estimate that approximately 250 chromophores reside inside the gap and contribute to the signal. If the different spectra were due to photofragments, all molecules in one resonator should undergo the same photoreaction. At the same time, the photoreactions in different resonators would be different. Furthermore, the stability of individual resonators was studied under typical experimental conditions (see Supporting Information, Figure S10). No changes were seen for the intensities and integration times used in the experiment.

We note that, in spite of strong individual variations, the ensemble of investigated resonators shows some effects which are in agreement with the predic-

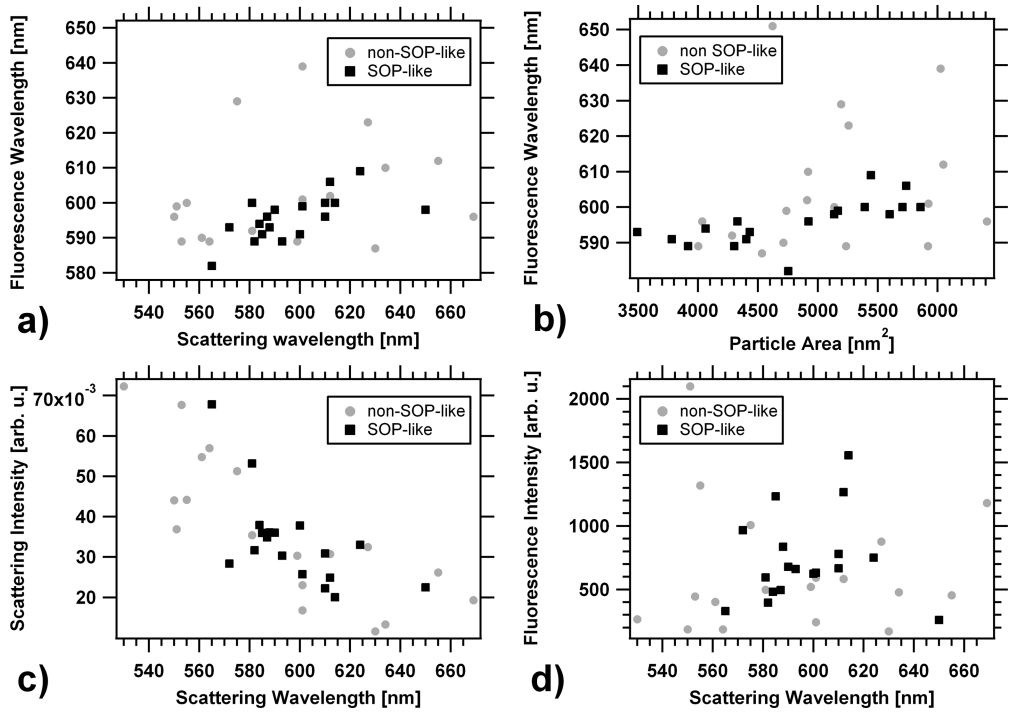

Figure 5. Correlation plots: (a) fluorescence wavelength versus scattering wavelength, (b) fluorescence wavelength versus particle area, (c) scattering intensity versus scattering wavelength, and (d) fluorescence intensity versus scattering wavelength. The two classes, SOP-like and non-SOP-like resonators, are marked with different symbols.

tions of "classical" fluorescence enhancement. They can be observed by correlating characteristic parameters that are obtained from the scattering and fluorescence spectra and electron microscopy. We consider the maximum fluorescence intensity, the wavelength where the maximum is seen, the maximum scattering intensity, the related wavelength, and the particle area. Plots of all 10 possible combinations of these parameters are shown in the Supporting Information, Figure S15. In many cases, no clear trend is seen. Figure 5 shows four combinations where we see a trend. In Figure 5a, the wavelength of the scattering maximum correlates with the wavelength of the fluorescence maximum. This is expected of plasmonic resonators with a wavelength-dependent emission enhancement which roughly coincides with the scattering spectrum. Despite some scatter, the correlation for the SOP-like resonators is obvious. Such behavior could already be inferred from Figure 3a−c, where the wavelength of maximum fluorescence emission follows the scattering maximum. For the non-SOP-like resonators, strong individual differences are seen, indicating that a description in terms of a one-to-one correspondence between the scattering spectrum and the enhancement spectrum is too simplified. The variation between the individuals can be partly assigned to the different sizes of the silver particles (area from 3500 to 6400 nm^2). This is evident from a weak correlation between the particle size and the wavelengths of maximum fluorescence and scattering, as seen in Figure 5b. A considerable scatter in the data, in particular for the non-SOP cases, points to additional factors, *e.g.*, the nanostructure in the gap region influencing the plasmonic resonance. In Figure 5c we see a decrease in the scattering intensity with increasing wavelength. This is a consequence of the wavelength-dependent sensitivity of the dark-field microscopy using the intermediate excitation of surface plasmons in the film for enhancement.[34] In Figure 5d an efficient enhancement of the fluorescence is seen for scattering wavelengths between 600 and 620 nm, which correspond to the emission of the free PDI-G2 in solution. From these correlations one can get some impression of the information an ensemble experiment would provide. Here, the strong individual differences would be averaged out, and only comparably weak trends would be visible.

SUMMARY AND OUTLOOK

We have presented a well-defined silver sphere-on-plane system where a perylene diimide dye could be placed in a defined position between a silver sphere and a silver plane due to the rigidity and shape persistency of the dendrimer shell. It allowed us to study the fluorescence behavior of the dye in the resulting gap on a single object basis. The fluorescence was quenched on the metallic film, while a strong signal could be seen for each particle position. The fluorescence emission profile was modified and showed a significant emission on the blue side, which we assigned to hot luminescence. The maximum fluorescence emission peak shifted along with the scattering maximum of the plasmonic resonance. From the scattering response, two

classes of resonators could be distinguished. We could identify SOP-like resonators, roughly agreeing with theoretical calculations assuming a perfect geometry. About half of all investigated objects were non-SOP-like and differed strongly from the ideal case. For the SOP-like resonators, a fundamental and higher order peaks in the scattering response could be seen. Their positions agreed with theory, while their FWHM was significantly broader than predicted. Strong modifications of the dye emission spectrum were observed which seemed to involve physical mechanisms beyond a simple wavelength-dependent enhancement factor.

In our future research we plan to resolve the origins of the resonance broadening and the geometrical reasons why a particular resonator behaves as "non-SOP-like". We will also perform experiments on the dye lifetimes in the gap to investigate the origins of the fluorescence profile modifications.

EXPERIMENTAL SECTION

Microscope glass slides (clean white, 1 mm thick, Menzel Gläser GmbH, Braunschweig, Germany) were cleaned by immersion in a 2% detergent solution (Hellmanex, Hellma GmbH & Co. KG, Müllheim, Germany) in ultrapure water (Milli-Q, 18.2 MΩ · cm, Millipore, Billerica, MA), followed by extensive rinsing with ultrapure water and ethanol (HPLC grade, Fisher Scientific, Leicestershire, United Kingdom). After 2 h in a tube furnace at 550 °C in a nitrogen atmosphere, 1.5 nm chromium particles (99.9%, Unicore Materials, Balzers, Lichtenstein) as adhesive and 50 nm silver particles (99.99% granulate, 2.0−3.0 mm, Balzers) were thermally evaporated (Balzers BLS 500) on the clean glass substrates.

Silver particles were synthesized following a procedure described by Suber:[41] 850 mg of silver nitrate ($AgNO_3$, for analysis, 99.8%, Honeywell Riedel-de Haen, Seelze, Germany) and 150 mg of Daxad-19 (sodium salt of polynaphthalene sulfonate formaldehyde condensate, mol wt 8000 g/mol, GEO Specialty Chemicals, Deer Park, TX) were dissolved in 25 mL of ultrapure water in a 50 mL round flask. After the solution was heated under stirring to 40 °C, 2.8 mL of concentrated nitric acid (69.7 wt %, Honeywell Riedel-de Haen) was added. A solution of 1300 mg of ascorbic acid in 5.5 mL of ultrapure water was then added drop by drop within 10 min. During this process the suspension changed from light brown to olive and to brown-green. The suspension was allowed to cool and stirred for a further 60 min. The resulting silver particles were centrifugated three times at 8000 rpm for 10 min (relative centrifugal force (RCF) = 8200*g*, 5810R centrifuge with fixed angle rotor F-34-6-38, Eppendorf, Hamburg, Germany). Each time, the supernatant liquid was removed and the solid dispersed again in 45 mL of ultrapure water. The particles prepared in that way had a mean diameter of 80 nm, as determined by scanning electron microscopy (SEM, Gemini 1530, Zeiss-LEO, Oberkochen, Germany), and were stable for months.

A spacer layer of the dye-loaded PDI-G2 dendrimer molecules was assembled next. The synthesis of this class of dendrimers in general[30,42,43] and of the compound used in particular[44] is described in detail elsewhere. For its deposition, the glass substrates with the evaporated silver film were immersed in a 2.5 μM PDI-G2 dendrimer solution in tetrahydrofuran (THF, puriss, p.a., stabilized, Sigma Aldrich, Steinheim, Germany) for 1.5 h. The substrates were subsequently rinsed with THF and dried with nitrogen. The films had a thickness of around 2−3 nm[44] and were stable for weeks.

The particles were deposited by centrifugation of the substrates with the suspension at 2500 rpm for 2 min (RCF = 800*g*, same rotor). For this purpose the substrates were placed one by one in a custom-made Teflon holder inside a metal centrifugation tube (diameter = 37 mm), and the suspension was added. The angle for the sample support was 15° relative to the vertical when built into the rotor. A sketch of the setup is available in the Supporting Information, Figure S1. This method is necessary due to the hydrophobic nature of the surface after addition of the PDI-G2 in conjunction with the aqueous silver suspension. Subsequently, the substrates were rinsed with ultrapure water and dried with nitrogen.

Directly before each measurement, the silver film was scratched with a cannula (0.6 × 50 mm) in the shape of an asymmetric cross with an opening angle of approximately 30° and scratch thickness of 20 μm to facilitate alignment of the optical and electron microscopes. The scratches on the surface are seen in both images, which are available in the Supporting Information, Figure S2. They fit perfectly together when comparing their position, distance, and opening angle.

Fluorescence spectra of individual nanoparticles were obtained using a self-made scanning confocal microscope (SCOM) with a suitable combination of filters and full beam illumination mode.[45] The setup was described before.[34] A schematic drawing of the illumination configuration is shown in the Supporting Information, Figure S4. Light from a 532 nm diode laser (pumped solid state Nd:YAG, GCL-005-L, Crysta-Laser, Reno, NV) in combination with a 532 nm line filter (XL08 532NB3, Omega Optical Inc., Brattleboro, VT) and a 620 nm short-pass filter (3RD620SP, Omega Optical Inc.) was used for illumination. In the detection pathway, a 532 nm notch (RazorEdge NF01-532U-25, Semrock, Rochester, USA) and 532 nm long pass filter (RazorEdge LP03-532RU-25, Semrock) blocked all of the illumination light. The remaining fluorescence light was analyzed by a fiber-coupled CCD spectrometer (Andor Shamrock, SR303i, Andor Technology, Belfast, Northern Ireland). During measurement, the sample was exposed to a constant flow of nitrogen in order to avoid oxidation of the spacer layer. The spectra were compared with the emission spectra of PDI-G2 in solution (presented in the Supporting Information, Figure S5, obtained with a Tidas FI-3095 S spectrometer, J&M Analytik AG, Aalen, Germany).

For scattering spectroscopy, a plasmon-mediated dark-field mode was used with the same fiber-coupled CCD spectrometer. It was optimized for high quality dark-field images through metallic films.[34] The setup was slightly modified compared to the one described there, and only one block between the microscope objective and beam splitter was used. A xenon lamp (Osram XBO 150) served as an illumination source, and the light in the illumination pathway was linearly polarized (thin sheet polarizer 80 in rotary mount, LINOS Photonics GmbH & Co. KG, Germany) perpendicular to the aperture block and in the detection pathway parallel to it (PGT 2.15, Glan-Thompson polarizing prism, Bernhard Halle Nachfolger GmbH, Berlin, Germany).

The nanoparticles were imaged by scanning electron microscopy (SEM, LEO Gemini 1530, Zeiss, Oberkochen, Germany) with an acceleration voltage of 2 kV and an in-lense detector. Images were taken at lower magnification of approximate 6000× to locate the region of interest at the scratches and align the SEM field with the optical dark-field and fluorescence images. Once the locations of the nanoparticles were confirmed, the magnification was increased to 200000× to capture high-resolution images of the desired particles. The size of each analyzed particle was determined with the aid of image processing software by counting the pixels representing the particle in the 8-bit grayscale image and multiplying it by the pixel area in nanometer squares provided by the SEM.

Acknowledgment. M.S. acknowledges valuable discussions with Dr. Adriana Rueda. We thank Gunnar Glasser for his support in electron microscopy and GEO Specialty Chemicals for donating a large amount of the DAXAD 19. We acknowledge financial support from the Deutsche Forschungsgemeinschaft (DFG, SFB 625).

Supporting Information Available: Information about the centrifugation process, schematic representation of the used confo-

cal microscope, corresponding scanning electron and confocal images, the emission spectrum of the dye in solution, the polarization dependence of the scattering patterns, emission spectra of all investigated particles, the peak positions of all emission spectra, reproducibility of the spectra for a different excitation wavelength of 514 nm, polarizabilities for different dielectric functions, all correlation plots, an estimation of the intensity change compared to the free dye, and information on how the enhancement factors were determined. This material is available free of charge *via* the Internet at http://pubs.acs.org.

REFERENCES AND NOTES

1. Kneipp, K.; Moskovits, M.; Kneipp, H. *Surface-Enhanced Raman Scattering: Physics and Applications*, 1st ed.; Springer: Berlin, 2006; Vol. 103.
2. Xu, H. X.; Wang, X. H.; Persson, M. P.; Xu, H. Q.; Kall, M.; Johansson, P. Unified Treatment of Fluorescence and Raman Scattering Processes near Metal Surfaces. *Phys. Rev. Lett.* **2004**, *93*, 243002/1–243002/4.
3. Aslan, K.; Gryczynski, I.; Malicka, J.; Matveeva, E.; Lakowicz, J. R.; Geddes, C. D. Metal-Enhanced Fluorescence: An Emerging Tool in Biotechnology. *Curr. Opin. Biotechnol.* **2005**, *16*, 55–62.
4. Lakowicz, J. R. Radiative Decay Engineering: Biophysical and Biomedical Applications. *Anal. Biochem.* **2001**, *298*, 1–24.
5. Fedutik, Y.; Temnov, V. V.; Schops, O.; Woggon, U.; Artemyev, M. V. Exciton-Plasmon-Photon Conversion in Plasmonic Nanostructures. *Phys. Rev. Lett.* **2007**, *99*, 136802/1–136802/4.
6. Koller, D. M.; Hohenau, A.; Ditlbacher, H.; Galler, N.; Aussenegg, F. R.; Leitner, A.; Krenn, J. R.; Eder, S.; Sax, S.; List, E. J. W. Surface Plasmon Coupled Electroluminescent Emission. *Appl. Phys. Lett.* **2008**, *92*, 103304/1–103304/2.
7. Hayashi, S.; Kozaru, K.; Yamamoto, K. Enhancement of Photoelectric Conversion Efficiency by Surface-Plasmon Excitation—A Test with an Organic Solar-Cell. *Solid State Commun.* **1991**, *79*, 763–767.
8. Glass, M.; Liao, P. F.; Bergman, J. G.; Olson, D. H. Interaction of Metal Particles with Adsorbed Dye Molecules: Absorption and Luminescence. *Opt. Lett.* **1980**, *5*, 367–370.
9. Ritchie, G.; Burstein, E. Luminescence of Dye Molecules Adsorbed at a Ag Surface. *Phys. Rev. B* **1981**, *24*, 4843–4846.
10. Wokaun, A. Surface Enhancement of Optical Fields Mechanism and Applications. *Mol. Phys.* **1985**, *56*, 1–33.
11. Wokaun, A.; Lutz, H. P.; King, A. P.; Wild, U. P.; Ernst, R. R. Energy Transfer in Surface Enhanced Luminscence. *J. Chem. Phys.* **1983**, *79*, 509–514.
12. Barnes, W. L. Fluorescence near Interfaces: The Role of Photonic Mode Density. *J. Mod. Opt.* **1998**, *45*, 661–699.
13. Anger, P; Bharadwaj, P; Novotny, L. Enhancement and Quenching of Single-Molecule Fluorescence. *Phys. Rev. Lett.* **2006**, *96*, 113002/1–113002/4.
14. Kuhn, S; Hakanson, U; Rogobete, L; Sandoghdar, V. Enhancement of Single-Molecule Fluorescence Using a Gold Nanoparticle As an Optical Nanoantenna. *Phys. Rev. Lett.* **2006**, *97*, 017402/1–017402/4.
15. Rogobete, L.; Kaminski, F.; Agio, M.; Sandoghdar, V. Design of Plasmonic Nanoantennae for Enhancing Spontaneous Emission. *Opt. Lett.* **2007**, *32*, 1623–1625.
16. Romero, I.; Aizpurua, J.; Bryant, G. W.; de Abajo, F. J. G. Plasmons in Nearly Touching Metallic Nanoparticles: Singular Response in the Limit of Touching Dimers. *Opt. Express* **2006**, *14*, 9988–9999.
17. Aravind, P. K.; Metiu, H. the Effects of the Interaction between Resonances in the Electromagnetic Response of a Sphere-on-Plane Structure—Applications to Surface Enhances Spectroscopy. *Surf. Sci.* **1983**, *124*, 506–528.
18. Nordlander, P.; Le, F. Plasmonic Structure and Electromagnetic Field Enhancements in the Metallic Nanoparticle-Film System. *Appl. Phys. B-Lasers Opt.* **2006**, *84*, 35–41.
19. Nordlander, P.; Prodan, E. Plasmon Hybridization in Nanoparticles near Metallic Surfaces. *Nano Lett.* **2004**, *4*, 2209–2213.
20. Zhao, J.; Sherry, L. J.; Schatz, G. C.; Van Duyne, R. P. Molecular Plasmonics: Chromophore-Plasmon Coupling and Single-Particle Nanosensors. *IEEE J. Sel. Top. Quantum Electron.* **2008**, *14*, 1418–1429.
21. Futamata, M. Single Molecule Sensitivity in SERS: Importance of Junction of Adjacent Ag Nanoparticles. *Faraday Discuss.* **2006**, 45–61.
22. Futamata, M.; Maruyama, Y.; Ishikawa, M. Critical Importance of the Junction in Touching Ag Particles for Single Molecule Sensitivity In SERS. *J. Mol. Struct.* **2005**, *735*, 75–84.
23. Trügler, A.; Hohenester, U. Strong Coupling between a Metallic Nanoparticle and a Single Molecule. *Phys. Rev. B, Condens, Matter Mater. Phys.* **2008**, *77*, 115403/1–115403/6.
24. Zuloaga, J.; Prodan, E.; Nordlander, P. Quantum Description of the Plasmon Resonances of a Nanoparticle Dimer. *Nano Lett.* **2009**, *9*, 887–891.
25. Garcìa de Abajo, F. J. Nonlocal Effects in the Plasmons of Strongly Interacting Nanoparticles, Dimers, and Waveguides. *J. Phys. Chem. C* **2008**, *112*, 17983–17987.
26. Vielma, J.; Leung, P. T. Nonlocal Optical Effects on the Fluorescence and Decay Rates for Admolecules at a Metallic Nanoparticle. *J. Chem. Phys.* **2007**, *126*, 194704/1–194704/7.
27. Kolb, D. M. *Spectroelectrochemistry: Theory and Practice*; Plenum: New York, 1988.
28. Vukovic, S.; Corni, S.; Mennucci, B. Fluorescence Enhancement of Chromophores Close to Metal Nanoparticles. Optimal Setup Revealed by the Polarizable Continuum Model. *J. Phys. Chem. C* **2009**, *113*, 121–133.
29. Wind, M.; Saalwachter, K.; Wiesler, U. M.; Mullen, K.; Spiess, H. W. Solid-State NMR Investigations of Molecular Dynamics in Polyphenylene Dendrimers: Evidence of Dense-Shell Packing. *Macromolecules* **2002**, *35*, 10071–10086.
30. Herrmann, A.; Weil, T.; Sinigersky, V.; Wiesler, U. W.; Vosch, T.; Hofkens, J.; De Schryver, F. C.; Müllen, K. Polyphenylene Dendrimers with Perylene Diimide as a Luminescent Core. *Chem.—Eur. J.* **2001**, *7*, 4844–4853.
31. Flors, C.; Oesterling, I.; Schnitzler, T.; Fron, E.; Schweitzer, G.; Sliwa, M.; Herrmann, A.; van der Auweraer, M.; de Schryver, F. C.; Mullen, K.; Hofkens, J. Energy and Electron Transfer in Ethynylene Bridged Perylene Diimide Multichromophores. *J. Phys. Chem. C* **2007**, *111*, 4861–4870.
32. Kohl, C.; Weil, T.; Qu, J. Q.; Mullen, K. Towards Highly Fluorescent and Water-Soluble Perylene Dyes. *Chem.—Eur. J.* **2004**, *10*, 5297–5310.
33. Sick, B.; Hecht, B.; Novotny, L. Orientational Imaging of Single Molecules by Annular Illumination. *Phys. Rev. Lett.* **2000**, *85*, 4482–4485.
34. Schmelzeisen, M.; Austermann, J.; Kreiter, M. Plasmon Mediated Confocal Dark-Field Microscopy. *Opt. Express* **2008**, *16*, 17826–17841.
35. Wind, M. M.; Vlieger, J.; Bedeaux, D. The polarizability of a truncated sphere on a substrate I. *Physica A: Statistical and Theoretical Physics* **1987**, *141*, 33–57.
36. Johnson, P. B.; Christy, R. W. Optical Constants of Noble-Metals. *Phys. Rev. B* **1972**, *6*, 4370–4379.
37. Lynch, D. W.; Huttner, W. R., *Handbook of Optical Constants of Solids*; Academic Press Inc.: San Diego, 1985; pp 275−367.
38. Rueda, A.; Vogel, N.; Kreiter, M. Characterization of Gold Films by Surface Plasmon Spectroscopy: Large Errors and Small Consequences. *Surf. Sci.* **2009**, *603*, 491–497.
39. Le Ru, E. C.; Etchegoin, P. G.; Grand, J.; Felidj, N.; Aubard, J.; Levi, G. Mechanisms of Spectral Profile Modification in Surface-Enhanced Fluorescence. *J. Phys. Chem. C* **2007**, *111*, 16076–16079.
40. Ringler, M.; Schwemer, A.; Wunderlich, M.; Nichtl, A.; Kurzinger, K.; Klar, T. A.; Feldmann, J. Shaping Emission Spectra of Fluorescent Molecules with Single Plasmonic

Nanoresonators. *Phys. Rev. Lett.* **2008**, *100*, 203002/1–203002/4.
41. Suber, L.; Sondi, I.; Matijevic, E.; Goia, D. V. Preparation and the Mechanisms of Formation of Silver Particles of Different Morphologies in Homogeneous Solutions. *J. Colloid Interface Sci.* **2005**, *288*, 489–495.
42. Qu, J.; Pschirer, N. G.; Liu, D.; Stefan, A.; De Schryver, F. C.; Müllen, K. Dendronized Perylenetetracarboxdiimides with Peripheral Triphenylamines for Intramolecular Energy and Electron Transfer. *Chem.—Eur. J.* **2004**, *10*, 528–537.
43. Qu, J.; Zhang, J.; Grimsdale, A. C.; Mullen, K.; Jaiser, F.; Yang, X.; Neher, D. Dendronized Perylene Diimide Emitters: Synthesis, Luminescence, and Electron and Energy Transfer Studies. *Macromolecules* **2004**, *37*, 8297–8306.
44. Rueda, A.; Stemmler, M.; Bauer, R.; Mullen, K.; Fogel, Y.; Kreiter, M. Optical Resonances of Gold Nanoparticles on a Gold Surface: Quantitative Correlation of Geometry and Resonance Wavelength. *New J. Phys.* **2008**, *10*, 113001/1–113001/21.
45. Stefani, F. D.; Vasilev, K.; Bocchio, N.; Stoyanova, N.; Kreiter, M. Surface-Plasmon-Mediated Single-Molecule Fluorescence through a Thin Metallic Film. *Phys. Rev. Lett.* **2005**, *94*, 023005/1–023005/4.